

Supplementary Material

Uranyl N₂O₂-Schiff Base Complex as Co-catalyst in Ethanol Electro-oxidation: Synthesis, Crystallographic, Spectroscopic, Electrochemical, and DFT Characterization, and Catalytic Investigation

Elizomar Medeiros Barbosa^a; Kaique Souza Soares^a; Thiago Henrique Döring^b, Igor Vinicius de França^b, Lucas dos S. Mello^c, Glaucio R. Nagurniak^d, Renato L. T. Parreira^e; Felipe T. Martins^f; Edward Ralph Dockal^c; Elson Almeida Souza^a; Paulo José Sousa Maia^{g*}; José Wilmo da Cruz Jr.*^b

^aInstituto de Ciências Exatas e tecnologia, Universidade Federal do Amazonas, Itacoatiara, AM, Brazil;

^bDepartamento de Ciências Exatas e Educação, Universidade Federal de Santa Catarina, Rua João Pessoa 2514, Blumenau, SC, Brazil;

^cDepartamento de Química, Universidade Federal de São Carlos, Rod. Washington Luiz, km 235, São Carlos, SP, Brazil;

^dDepartment of Chemistry, State University of Ponta Grossa, Ponta Grossa - PR, 84030-900, Brazil.

^eCenter of research in exact sciences and technologies, University of Franca, Franca - SP, 14404-600, Brazil.

^fUFG, Universidade Federal de Goiás, Instituto de Química, Goiânia - GO, 74690-900, Brazil.

^gGEOBio: Grupo de Eletrocatalise, Fotoquímica Inorgânica e Química Bioinorgânica, Instituto Multidisciplinar de Química, Centro Multidisciplinar

List of Tables

Table S1. ^1H (400 MHz) and ^{13}C (100 MHz) data of H_2L and $[\text{UO}_2(\text{L})\text{H}_2\text{O}]$ in $\text{DMSO}-d_6$ (25 °C) with tetramethylsilane (TMS), as internal standard (chemical shifts in ppm and J in Hz).....	4
Table S2. Experimental (190-800 nm, Acetonitrile, 25°C) and theoretical (ZORA-PBE/Def2-TZVPP-3BJ//SARC-TZVPP – SMD-Acetonitile) UV-Vis attribution (λ in nm and ϵ in $\text{L}^\bullet\text{mol}^{-1}\text{cm}^{-1}$)....	8

List of Figures

Figure S1. ^1H NMR spectrum (400 MHz, $\text{DMSO}-d_6$) of 3-OMe- <i>c</i> -salcn.	5
Figure S2. ^{13}C NMR spectrum (100 MHz, $\text{DMSO}-d_6$) of 3-OMe- <i>c</i> -salcn....	5
Figure S3. Infrared spectra (4000-450 cm^{-1} , KBr) $[\text{UO}_2(3\text{OMe-}c\text{-salcn})\text{H}_2\text{O}]$	6
Figure S4. ^1H NMR spectrum (400 MHz, $\text{DMSO}-d_6$) of $[\text{UO}_2(3\text{OMe-}c\text{-salcn})\text{H}_2\text{O}]$	6
Figure S5. ^{13}C NMR spectrum (400 MHz, $\text{DMSO}-d_6$) of $[\text{UO}_2(3\text{OMe-}c\text{-salcn})\text{H}_2\text{O}]$	7
Figure S6. Optimized geometry of <i>cis</i> - $[\text{UO}_2(3\text{-OMe-}c\text{-salcn})(\text{H}_2\text{O})]$ at DKH-PBE/Def2-TZVPP-D3BJ//SARC-TZVPP level of theory.....	7
Figure S7. Optimized geometry of <i>trans</i> - $[\text{UO}_2(3\text{-OMe-}c\text{-salcn})(\text{H}_2\text{O})]$ at DKH-PBE/Def2-TZVPP-D3BJ//SARC-TZVPP level of theory.....	8
Figure S8. $[\text{UO}_2(3\text{-OMe-}c\text{-salcn})\text{H}_2\text{O}]$ UV-Vis electronic spectra (200-800 nm, acetonitrile, 25°C).....	9
Figure S9. Gaussian analysis of $[\text{UO}_2(3\text{-OMe-}c\text{-salcn})\text{H}_2\text{O}]$ for electronic spectrum in the 50000-20000 cm^{-1} (200-500 nm, Acetonitrile, 25°C) region.....	10
Figure S10. UV-VIS spectrum of $[\text{UO}_2(3\text{-OMe-}c\text{-salcn})\text{H}_2\text{O}]$ calculated at ZORA-PBE/Def2-TZVPP-3BJ//SARC-TZVPP (SMD-acetonitrile) level of theory.....	10

- Figure S11. Molecular orbitals involved at calculated light absorption process of $[UO_2(3\text{-OMe-}c\text{-salcn})H_2O]$ at 1003 nm. 11
- Figure S12. Molecular orbitals involved at calculated light absorption process of $[UO_2(3\text{-OMe-}c\text{-salcn})H_2O]$ at 835 nm. 11
- Figure S13. Molecular orbitals involved at calculated light absorption process of $[UO_2(3\text{-OMe-}c\text{-salcn})H_2O]$ at 612 nm. 12
- Figure S14. Molecular orbitals involved at calculated light absorption processes of $[UO_2(3\text{-OMe-}c\text{-salcn})H_2O]$ around 411 nm. .. 13

Table S1. ^1H (400 MHz) and ^{13}C (100 MHz) data of H_2L and $[\text{UO}_2(\text{L})\text{H}_2\text{O}]$ in $\text{DMSO}-d_6$ (25°C) with tetramethylsilane (TMS), as internal standard (chemical shifts in ppm and J in Hz).

	H_2L	$[\text{UO}_2(\text{L})\text{H}_2\text{O}]$		
	δ ^1H (multiplicity, J Hz)	δ ^1H (multiplicity, J Hz)		
	δ ^{13}C	δ ^{13}C		
1	-	118.35	-	123.7
2	-	151.69	-	159.7
3	-	148.03	-	150.9
4	7.00 (m)	117.68	7.22 (dd, 7.8, 1.5)	116.5
5	6.79 (t, 7.88)	114.55	6.61 (t, 7.8)	115.4
6	7.00 (m)	123.21	7.25 (dd, 7.8, 1.5)	126.4
7	8.55 (s)	165.29	9.40 (s)	167.8
8	3.68 (d, 5.68)	67.75	4.63-4.55 (m)	70.6
9	1.80 (m), 1.55 (m)	30.42	2.40-2.20 (m)	27.5
10		21.91	1.88-1.72 (m) 1.68-1.58 (m)	21.4
11	3.74 (s)	55.62	3.97 (s)	56.1
OH	13.51 (s)	-	-	-

s = singlet, d = doublet, dd = doublet of doublets, t = triplet, m = multiplet.

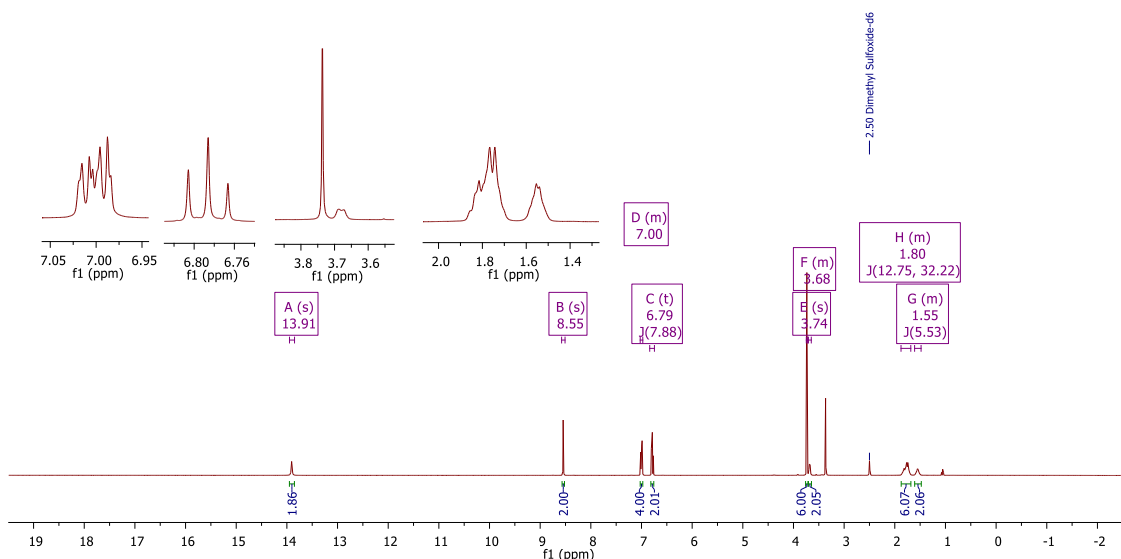


Figure S1. ^1H NMR spectrum (400 MHz, $\text{DMSO}-d_6$) for 3-OMe-*c*-salcn.

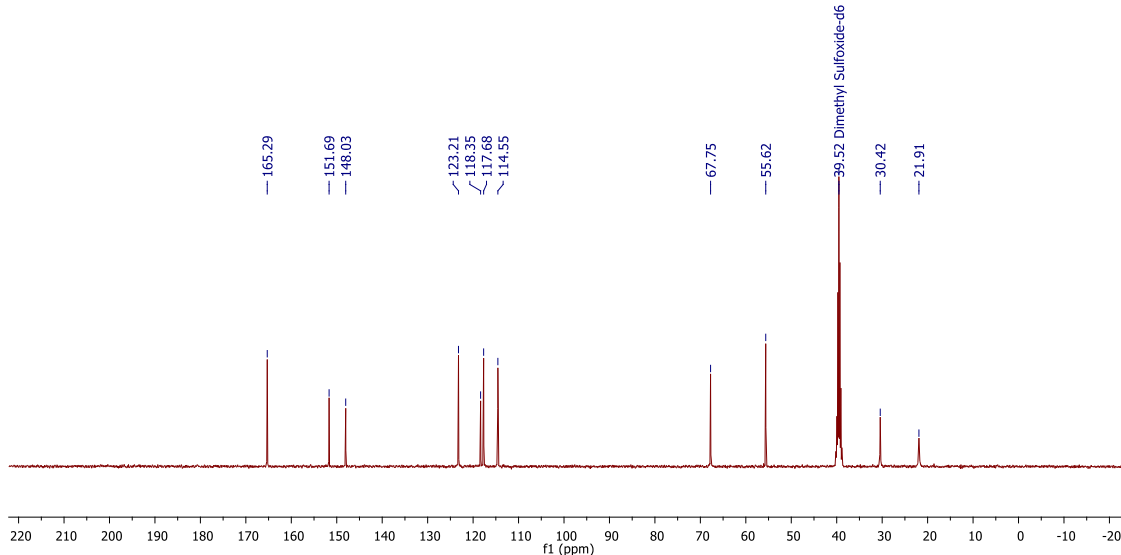


Figure S2. ^{13}C NMR spectrum (100 MHz, $\text{DMSO}-d_6$) for 3-OMe-*c*-salcn.

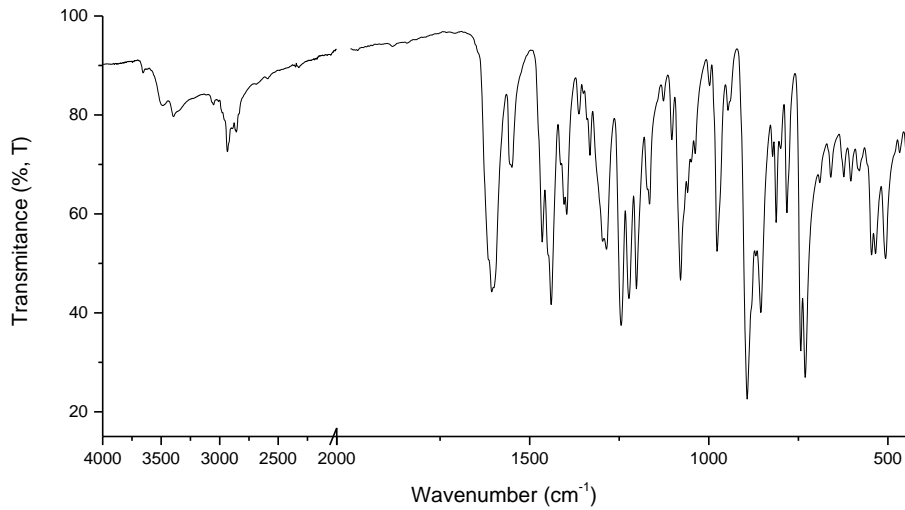


Figure S3. Infrared spectra (4000-450 cm^{-1} , KBr) for $[\text{UO}_2(30\text{Me}-c\text{-salcn})\text{H}_2\text{O}]$.

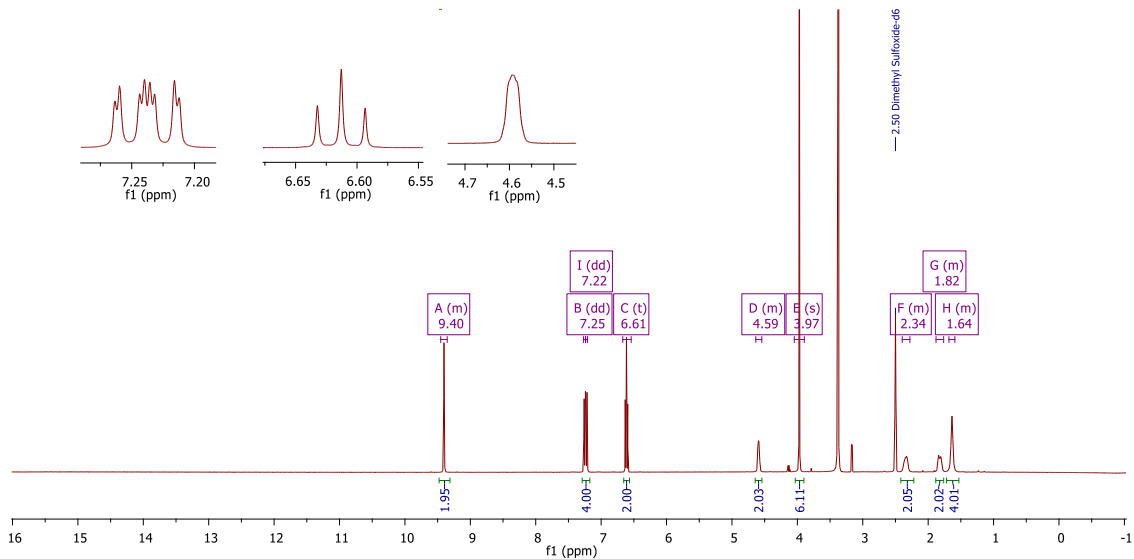


Figure S4. ^1H NMR spectrum (400 MHz, $\text{DMSO}-d_6$) for $[\text{UO}_2(30\text{Me}-c\text{-salcn})\text{H}_2\text{O}]$.

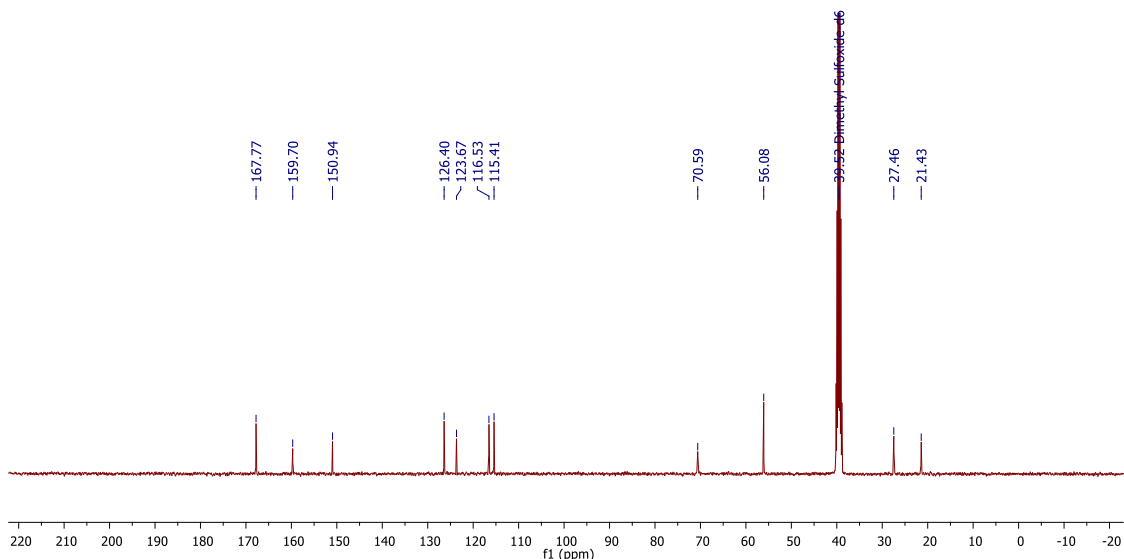


Figure S5. ^{13}C NMR spectrum (400 MHz, $\text{DMSO}-d_6$) for $[\text{UO}_2(3\text{OMe}-c\text{-salcn})\text{H}_2\text{O}]$.

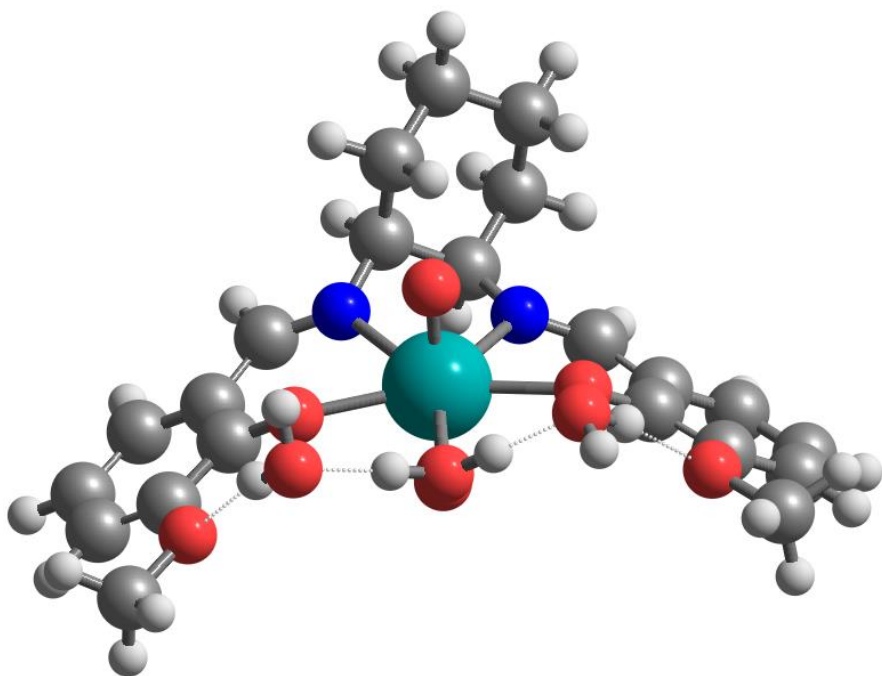


Figure S6. Optimized geometry for *cis*- $[\text{UO}_2(3\text{-OMe}-c\text{-salcn})(\text{H}_2\text{O})]$ at DKH-PBE/Def2-TZVPP-D3BJ//SARC-TZVPP level of theory.

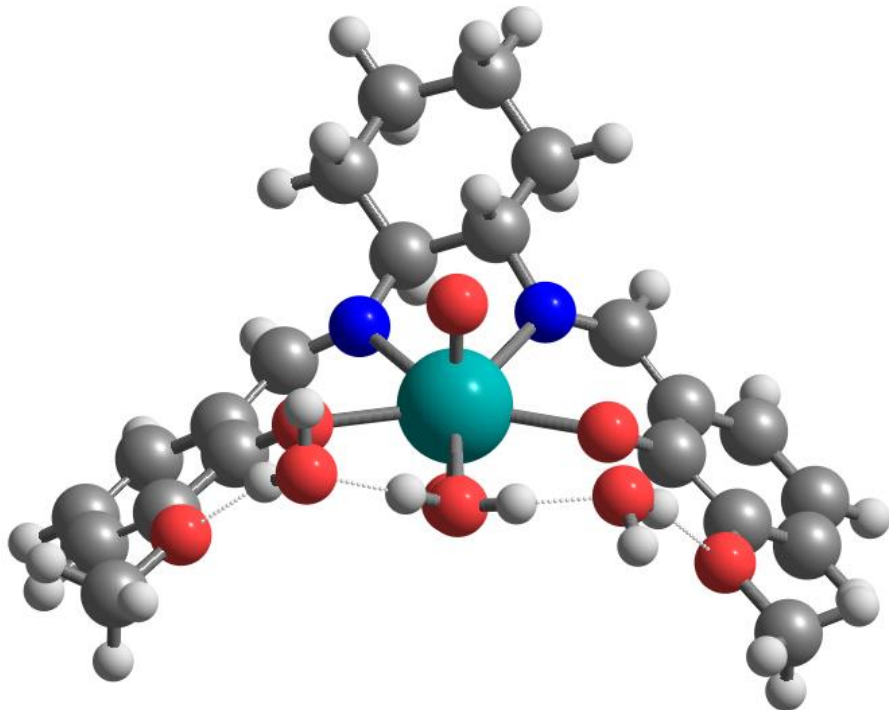


Figure S7. Optimized geometry for *trans*-[UO₂(3-OMe-*c*-salcn)(H₂O)] at DKH-PBE/Def2-TZVPP-D3BJ//SARC-TZVPP level of theory.

Table S2. Experimental (190-800 nm, Acetonitrile, 25°C) and theoretical (ZORA-PBE/Def2-TZVPP-3BJ//SARC-TZVPP – SMD-Acetonitrile) UV-Vis attribution (λ in nm and ϵ in L[•]mol⁻¹cm⁻¹).

Comp	Experimental				$\lambda_{\text{máx}}$	Assignment
	Observed	G. A				
	$\lambda_{\text{máx}}$	$\epsilon_{\text{máx}}$	$\lambda_{\text{máx}}$	$\epsilon_{\text{máx}}$		
[UO ₂ (L)H ₂ O]					1003	LMCT ($p\pi \rightarrow f\pi$)
					835	LMCT
					616	LMCT ($p\pi \rightarrow f\pi$)
						-
	344	7311	482	33		LMCT ($p\pi \rightarrow f\pi$)
			401	1900	411	$\pi \rightarrow \pi^*$

		347	4400	LMCT
		282	10300	LMCT
268	21500	268	8800	$\pi \rightarrow \pi^*(N=C)$
		239	31600	$\pi \rightarrow \pi^*(C=C)$
236	61000	229	35900	$\pi \rightarrow \pi^*(C=C)$

G.A - Gaussian analysis

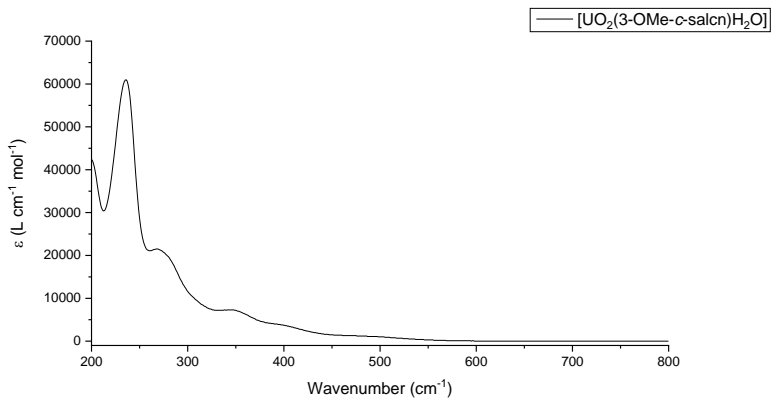


Figure S8. $[\text{UO}_2(3\text{-OMe-}c\text{-salcn})\text{H}_2\text{O}]$ UV-Vis electronic spectra (200-800 nm, acetonitrile, 25°C).

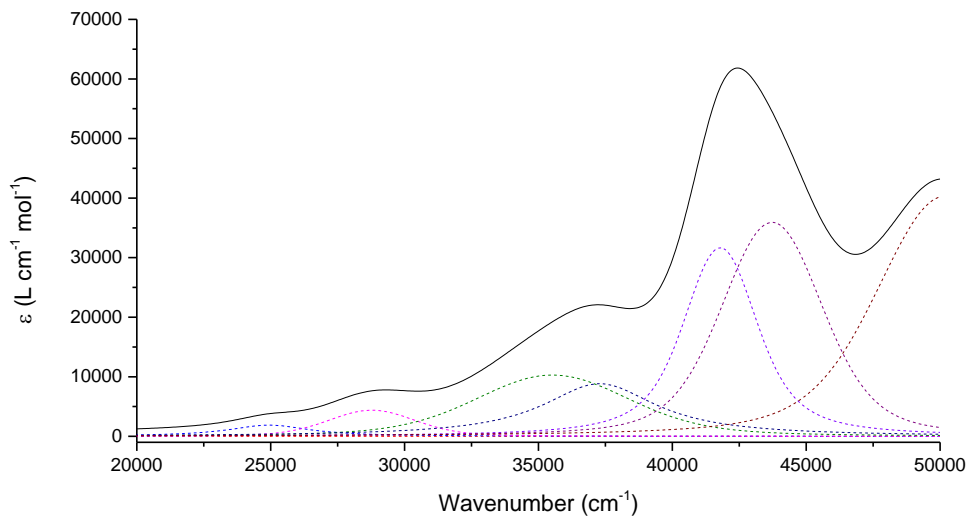


Figure S9. Gaussian analysis of $[UO_2(3\text{-OMe-}c\text{-salcn})H_2O]$ for electronic spectrum in the 50000-20000 cm^{-1} (200-500 nm, Acetonitrile, 25°C) region.

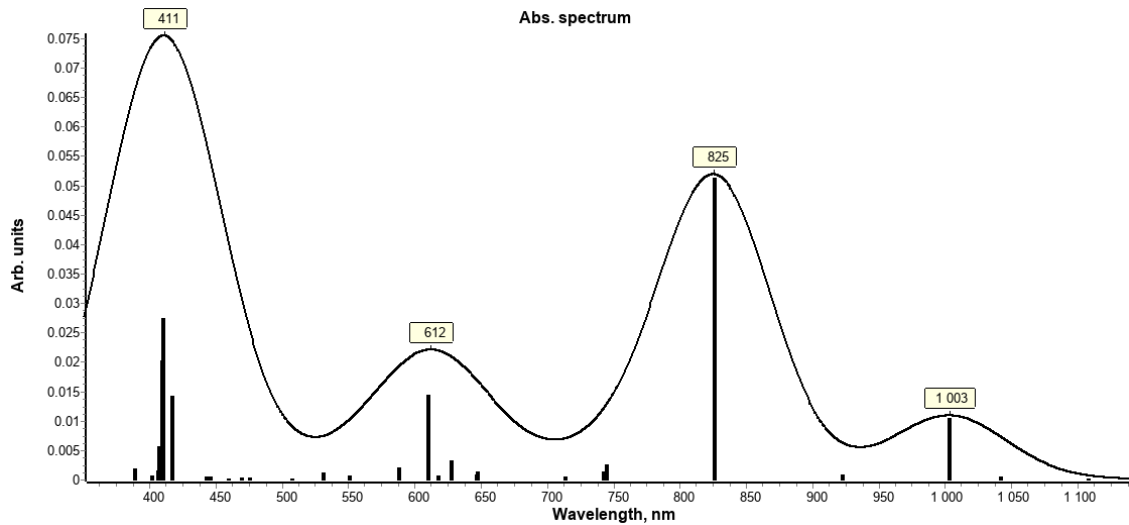


Figure S10. UV-VIS spectrum for $[UO_2(3\text{-OMe-}c\text{-salcn})H_2O]$ calculated at ZORA-PBE/Def2-TZVPP-3BJ//SARC-TZVPP (SMD-acetonitrile) level of theory.

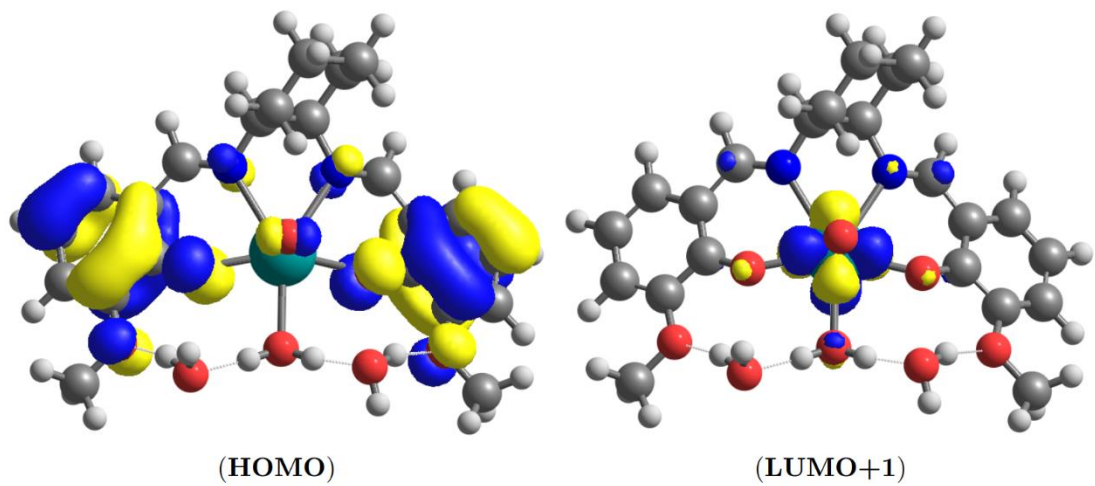


Figure S11. Molecular orbitals involved at calculated light absorption process of $[UO_2(3\text{-OMe-}c\text{-salcn})H_2O]$ at 1003 nm.

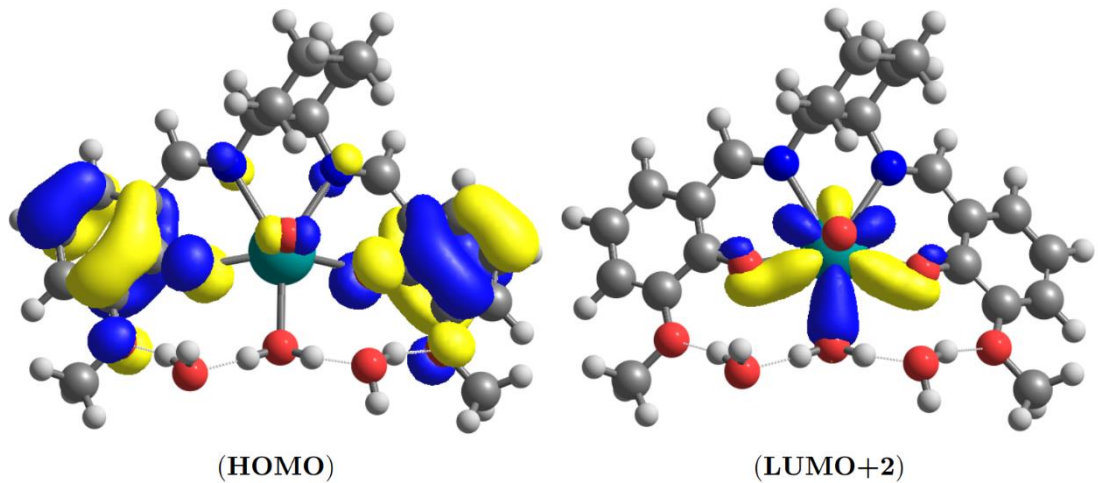


Figure S12. Molecular orbitals involved at calculated light absorption process of $[UO_2(3\text{-OMe-}c\text{-salcn})H_2O]$ at 835 nm.

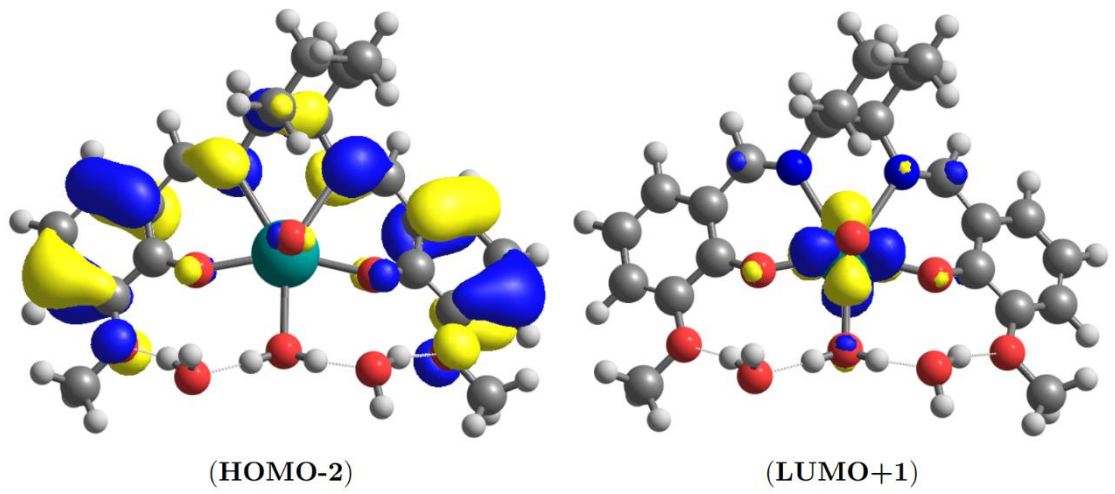
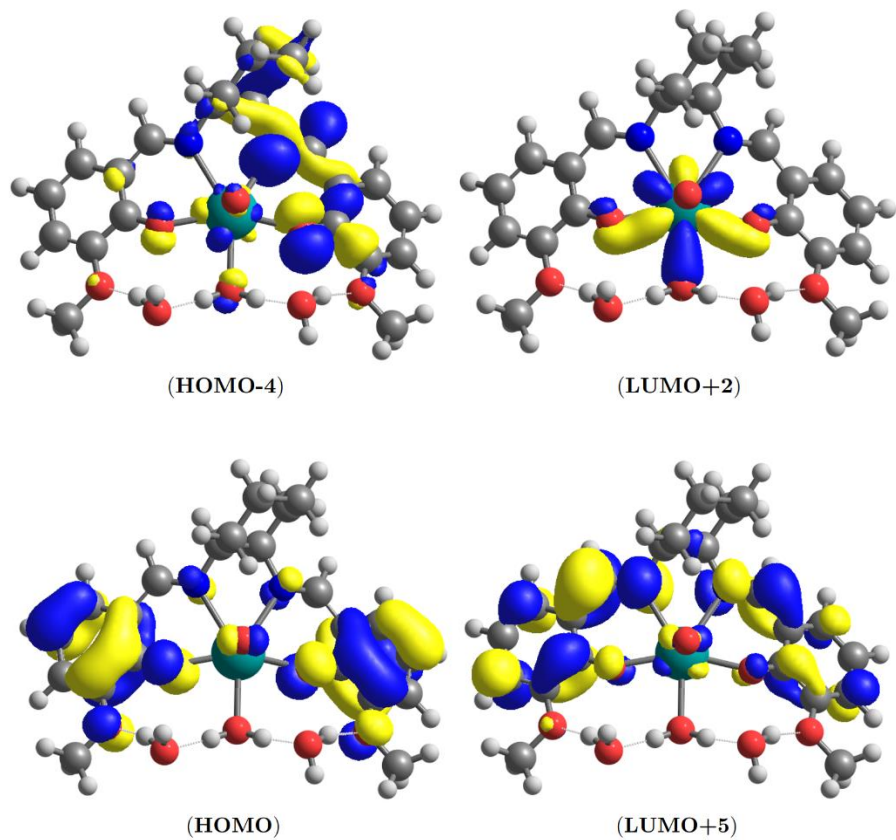


Figure S13. Molecular orbitals involved at calculated light absorption process of $[\text{UO}_2(3\text{-OMe-}c\text{-salcn})\text{H}_2\text{O}]$ at 612 nm.



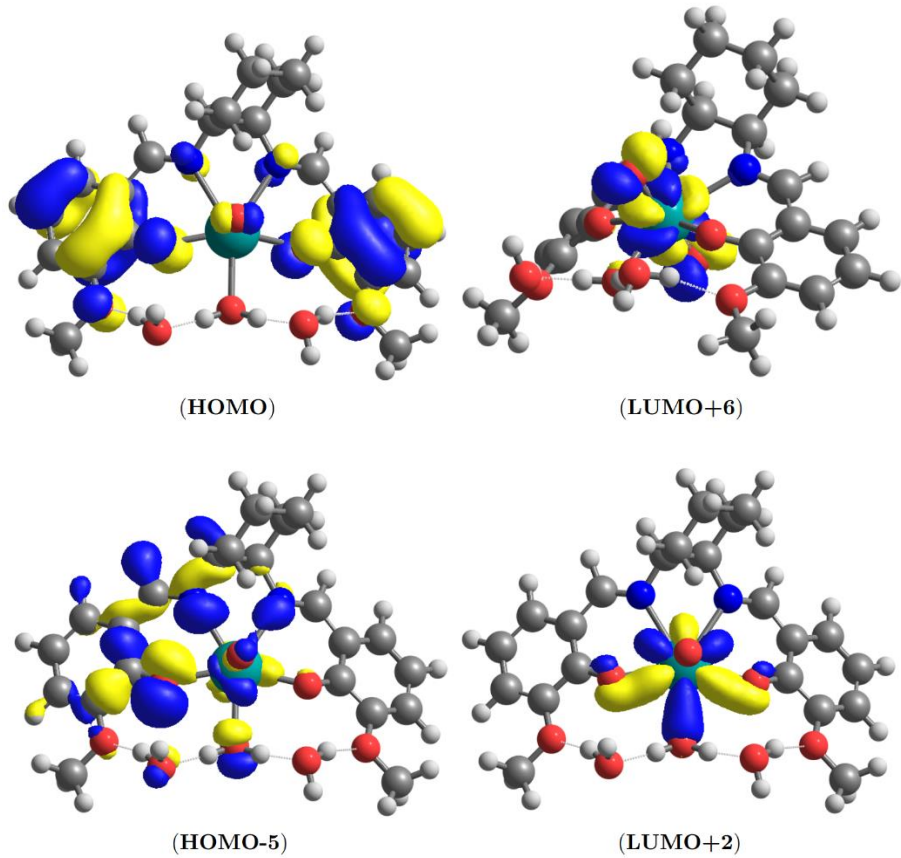


Figure S14. Molecular orbitals involved at calculated light absorption processes of $[\text{UO}_2(3\text{-OMe-}c\text{-salcn})\text{H}_2\text{O}]$ around 411 nm.